MAGNETIC PROPERTIES OF THIN FILM WITH $S = 1$. ISOTHERMAL SUSCEPTIBILITY AND MAGNETIC SPECIFIC HEAT

M. Gzik and T. Balcerzak

Solid State Physics Department, University of Łódź
Pomorska 149/153, 90-236 Łódź, Poland

(Received January 31, 1997; revised version April 21, 1997)

The thermodynamic response functions were studied in thin films in the frame of the Blume–Emery–Griffiths model. The method is based on the analysis of the Gibbs free energy and involves calculations of the magnetization and quadrupolar moment distributions. The temperature dependencies of the susceptibility and specific heat are obtained for various biquadratic interaction parameter and non-zero single-ion anisotropy. The behaviour of these functions in different phases: ferromagnetic, paramagnetic and staggered quadrupolar are illustrated in figures and discussed.

PACS numbers: 64.60.–i, 75.10.–b, 75.70.–i

1. Introduction

In the last years, many papers have been devoted to Blume–Emery–Griffiths (BEG) model for spin $S = 1$ [1–25]. The BEG model contains, besides the usual exchange interaction, the terms describing biquadratic interactions of spins and single-ion anisotropy. When these terms are competing with the exchange interactions they can lead to very interesting and rich phase diagrams. For instance, one can predict the existence of tricritical points (TCP), separating the continuous and discontinuous phase transitions [2–4, 6–10, 13–17, 20, 21, 24, 25], the occurrence of staggered quadrupolar phase [2–4, 6, 9, 12, 14, 16, 20, 24, 25] and the re-entrant magnetism phenomenon [6, 8, 9–11, 15, 16, 24, 25].

In the literature the following techniques have been applied to studies of BEG model: the molecular field approximation (MFA) [1, 2, 9, 15, 20, 24, 25] and other effective field methods [4, 6–8, 17, 23], renormalization group (RG) approach [13], cluster variational method (CVM) [5, 10–12, 16, 20, 21], coherent anomaly method (CAM) [18], variational cumulant expansion (VCE) [19] and Monte Carlo simulations [2, 3, 14, 22].

The BEG model has been applied to the description of bulk materials [3, 5, 7, 13, 16–18, 20], planar ferromagnets [2, 4, 6–8, 12–14, 20], semi-infinite

systems [11, 21], as well as the linear chains [22, 23]. Recently, an attempt was made to apply this model to the thin film [20, 24, 25]. However, these papers are still not numerous, and the authors have only studied the phase diagrams and the order parameters in different phases.

The aim of the present paper is to calculate the isothermal susceptibility and magnetic contribution to the specific heat for thin film in the frame of BEG model. As far as we know from literature such studies have not been done yet, therefore, to begin with, we choose the simplest molecular field approach.

The present paper is essentially the continuation of the work [24], where in the frame of MFA the phase diagrams, magnetization distribution, as well as the quadrupolar moments in the thin films have been calculated. It is worth noticing here that all the thermodynamic quantities (both calculated in [24] and in the present work as well) have been obtained from one basic expression for the Gibbs free energy of the film remaining in equilibrium. Such approach ensures the internal self-consistency of the theory, i.e., it gives the proper relationships between different thermodynamic quantities, and yields the criterion for the correct decision which of various possible solutions are physical. The decisive factor is then the value of the Gibbs free energy, which for the physical solution should be in a minimum.

In the theoretical part of this paper we will derive the formula for the isothermal susceptibility and the magnetic specific heat in BEG model for the thin film with an arbitrary thickness. We will assume that the film has simple cubic (sc) structure, consisting of two mutually interpenetrating sublattices. Such a model enables the discussion of staggered quadrupolar phase, in which the magnetic susceptibility and the specific heat are of particular interest.

Thin film equations are next solved numerically in the third section, and the results are shown in the figures. We will illustrate particularly those situations which correspond to some characteristic features of the phase diagram obtained in our previous paper [24].

The numerical results of temperature dependencies of the susceptibility and specific heat are discussed for an exemplary film with $n = 5$ atomic planes and different biquadratic interaction strength parameter. The confirmation for the important role of biquadratic interactions (when they are competitive to the bilinear exchange coupling) and especially their remarkable influence on thermodynamic response functions in thin film was found.

2. Theory

2.1. The free energy and magnetization

The anisotropic BEG Hamiltonian for the thin films is of the form

$$\mathcal{H} = -\frac{1}{2}J \sum_{\nu i,\mu j} S_{\nu i}S_{\mu j} - \frac{1}{2}A \sum_{\nu i,\mu j} (S_{\nu i}S_{\mu j})^2 - D\sum_{\nu i} S_{\nu i}^2 - h\sum_{\nu i} S_{\nu i}, \qquad (1)$$

where $S_{\nu i} = \pm 1, 0$. We denote by J the exchange integral, whereas A and D parameters correspond to the biquadratic interactions and single-ion anisotropy, respectively. In Eq. (1), h stands for the external magnetic field. The indices

$\nu, \mu = 1, 2, \ldots, n$ denote the layer numbers, whereas $i, j = 1, 2, \ldots, N$ number the lattice site within a particular layer.

The Gibbs free energy can be calculated with the help of the Bogolyubov inequality

$$G(\mathcal{H}) \leq G(\mathcal{H}^0) + \langle \mathcal{H} - \mathcal{H}^0 \rangle_0, \tag{2}$$

where $\mathcal{H}^0$ stands for a trial Hamiltonian, which in MFA is given by the formula

$$\mathcal{H}^0 = -J \sum_{\nu i} S_{\nu i} \Lambda_{\nu i} - A \sum_{\nu i} S_{\nu i}^2 K_{\nu i} - D \sum_{\nu i} S_{\nu i}^2 - h \sum_{\nu i} S_{\nu i}. \tag{3}$$

The averaging symbol in Eq. (2), $\langle \ldots \rangle_0$ denotes the statistical averaging with the trial Hamiltonian. The parameters $\Lambda_{\nu i}$ and $K_{\nu i}$ in $\mathcal{H}^0$ represent the molecular fields of exchange and biquadratic interactions, respectively.

By minimization of the functional $G(\{\Lambda_{\nu i}\}, \{K_{\nu i}\})$ with respect to $\Lambda_{\nu i}$ and $K_{\nu i}$ parameters one can obtain the expressions for the equilibrium magnetizations m_ν^l and the quadrupolar moments q_ν^l given by the definitions

$$m_\nu^l = (\langle S_{\nu l} \rangle_0)_{\text{eq}} \qquad \text{and} \qquad q_\nu^l = \left(\langle S_{\nu l}^2 \rangle_0\right)_{\text{eq}}. \tag{4}$$

In Eqs. (4) $l = a, b$ denotes one of two interpenetrating sublattices. The assumption concerning two sublattices structure is necessary for the discussion of staggered quadrupolar phase in $S = 1$ system.

As it has been shown in the papers [24, 25], the magnetization distribution and the quadrupolar moments in thin film are given by the set of mutually coupled equations. They can be written as follows:

$$m_\nu^l = 2\left(1 - q_\nu^l\right) \exp\left[\beta\left(AQ_\nu^l + D\right)\right] \sinh\left[\beta\left(JM_\nu^l + h\right)\right] \tag{5}$$

and

$$q_\nu^l = 2\left(1 - q_\nu^l\right) \exp\left[\beta\left(AQ_\nu^l + D\right)\right] \cosh\left[\beta\left(JM_\nu^l + h\right)\right], \tag{6}$$

where $\beta = 1/k_{\text{B}}T$.

The Gibbs free energy of the thin film in equilibrium, per one lattice site and expressed in J constant units, is then of the form

$$\frac{G}{NnJ} = -\frac{1}{2n} y \sum_{l=a,b} \sum_{\nu=1}^{n} \ln\left\{2 \exp\left[\frac{1}{y}\left(\frac{A}{J} Q_\nu^l + \frac{D}{J}\right)\right] \cosh\left[\frac{1}{y}\left(M_\nu^l + \frac{h}{J}\right)\right] + 1\right\}$$

$$+ \frac{1}{4n} \sum_{l=a,b} \sum_{\nu=1}^{n} \left(m_\nu^l M_\nu^l + \frac{A}{J} q_\nu^l Q_\nu^l\right), \tag{7}$$

where

$$y = k_{\text{B}}T/J \tag{8}$$

denotes a dimensionless temperature and the molecular fields M_ν^l and Q_ν^l are then given by

$$M_\nu^l \equiv (\Lambda_{\nu l})_{\text{eq}} = z_{\nu,\nu} m_\nu^{a+b-l} + z_{\nu,\nu-1} m_{\nu-1}^{a+b-l} + z_{\nu,\nu+1} m_{\nu+1}^{a+b-l} \tag{9}$$

and

$$Q_\nu^l \equiv (K_{\nu l})_{\text{eq}} = z_{\nu,\nu} q_\nu^{a+b-l} + z_{\nu,\nu-1} q_{\nu-1}^{a+b-l} + z_{\nu,\nu+1} q_{\nu+1}^{a+b-l}. \tag{10}$$

According to definitions contained in Eqs. (9) and (10), M_ν^l and Q_ν^l are the variational parameters taken in equilibrium, for which the G-functional has its minimum. By $z_{\nu,\nu}$ we denote here the number of nearest neighbours of the spin $S_{\nu i}$ from the same ν-th plane, whereas $z_{\nu,\nu\pm1}$ is the number of its nearest neighbours from $(\nu \pm 1)$-th plane. For instance, for simple cubic lattice $z_{\nu,\nu} = 4$ for $\nu = 1, 2, \ldots, n$ whereas $z_{\nu,\nu\pm1} = 1$ inside the film ($\nu = 2, 3, \ldots, n-1$) and $z_{1,0} = z_{n,n+1} = 0$ at the surfaces.

From the analysis of the Gibbs free energy (7) one can derive all thermodynamic properties of the system, in particular, the isothermal susceptibility χ_T and the magnetic specific heat C_h at $h = \text{const}$.

2.2. The isothermal susceptibility

The magnetic isothermal susceptibility of the system is defined as the second derivative of the Gibbs free energy, when $T = \text{const}$.

$$\chi_T = -\left(\frac{\partial^2 G}{\partial h^2}\right)_T = \left(\frac{\partial M}{\partial h}\right)_T . \tag{11}$$

In Eq. (11) M denotes the total magnetization of the thin film, being a sum of two sublattice magnetizations from all n atomic planes.

$$M = \frac{N}{2}\sum_{\nu=1}^{n}\left(m_\nu^a + m_\nu^b\right), \tag{12}$$

where m_ν^a and m_ν^b are given by the formulae (5) and (6).

Now then, in order to calculate the susceptibility one has to determine the derivatives $\left(\partial m_\nu^l/\partial h\right)_T$. They can be obtained after differentiating the set of Eqs. (5) and (6). Performing differentiation with respect to h we get the set of linear equations for the derivatives in the following form:

$$q_\nu^l\left(\frac{\partial m_\nu^l}{\partial h}\right)_T - m_\nu^l\left(\frac{\partial q_\nu^l}{\partial h}\right)_T = \left[\left(q_\nu^l\right)^2 - \left(m_\nu^l\right)^2\right]\beta\left[J\left(\frac{\partial M_\nu^l}{\partial h}\right)_T + 1\right], \tag{13}$$

$$\left[q_\nu^l - \left(m_\nu^l\right)^2\right]\left(\frac{\partial q_\nu^l}{\partial h}\right)_T - m_\nu^l\left(1 - q_\nu^l\right)\left(\frac{\partial m_\nu^l}{\partial h}\right)_T$$

$$= \left(1 - q_\nu^l\right)\left[\left(q_\nu^l\right)^2 - \left(m_\nu^l\right)^2\right]\beta A\left(\frac{\partial Q_\nu^l}{\partial h}\right)_T . \tag{14}$$

As it is seen, from (13) and (14), also derivatives $\left(\partial q_\nu^l/\partial h\right)_T$ can be obtained simultaneously with the derivatives $\left(\partial m_\nu^l/\partial h\right)_T$. The m_ν^l and q_ν^l in Eqs. (13) and (14) are treated as the parameters, which for a given temperature are known from Eqs. (5) and (6). It is worth noticing here that in some cases the set of Eqs. (5) and (6) may have more than one solution for the same temperature. These solutions can correspond to the paramagnetic, ferromagnetic or staggered quadrupolar phases. However, among these solutions the physical one is that corresponding to the lowest Gibbs energy. As pointed out in the papers [24] and [25], this is the only criterion for choosing the proper solution of the set (5) and (6).

In order to perform the numerical calculations we must express the susceptibility in dimensionless units and therefore instead of the derivatives $(\partial m_\nu^l/\partial h)_T$ and $(\partial q_\nu^l/\partial h)_T$, rather the following quantities should be used:

$$\chi_\nu^l \equiv \left(\frac{\partial m_\nu^l}{\partial(h/J)}\right)_T, \tag{15}$$

$$\eta_\nu^l \equiv \left(\frac{\partial q_\nu^l}{\partial(h/J)}\right)_T. \tag{16}$$

Then, the set of Eqs. (13) and (14) takes the form

$$\left[(q_\nu^i)^2 - (m_\nu^i)^2\right]\left[z_{\nu,\nu}\chi_\nu^j + z_{\nu,\nu+1}\chi_{\nu+1}^j + z_{\nu,\nu-1}\chi_{\nu-1}^j\right] - yq_\nu^i\chi_\nu^i + ym_\nu^i\eta_\nu^i$$
$$= -\left[(q_\nu^i)^2 - (m_\nu^i)^2\right], \tag{17}$$

$$\frac{A}{J}(1-q_\nu^i)\left[(q_\nu^i)^2 - (m_\nu^i)^2\right]\left[z_{\nu,\nu}\eta_\nu^j + z_{\nu,\nu+1}\eta_{\nu+1}^j + z_{\nu,\nu-1}\eta_{\nu-1}^j\right]$$
$$+ym_\nu^i(1-q_\nu^i)\chi_\nu^i - y\left[q_\nu^i - (m_\nu^i)^2\right]\eta_\nu^i = 0, \tag{18}$$

where $i = a, b$; $j = a + b - i$, and $y = k_B T/J$ is the dimensionless temperature. After solving Eqs. (17) and (18) the dimensionless isothermal susceptibility χ_T per one lattice site can be found from the formula

$$\frac{J}{Nn}\chi_T = \frac{1}{2n}\sum_{\nu=1}^{n}(\chi_\nu^a + \chi_\nu^b), \tag{19}$$

where χ_ν^l, for $l = a, b$, is the sublattice susceptibility in the ν-th layer, n is the number of layers and N stands for the number of atoms within each atomic plane.

2.3. The magnetic contribution to the specific heat

In the next step we will calculate the magnetic specific heat C_h at the constant field $h = \text{const}$. The specific heat, which is the thermal response function of a system, is defined as follows:

$$C_h = T\left(\frac{\partial S}{\partial T}\right)_h = -T\left(\frac{\partial^2 G}{\partial T^2}\right)_h, \tag{20}$$

where by S we denote the entropy

$$S = -\left(\frac{\partial G}{\partial T}\right)_h. \tag{21}$$

According to the definition (21) and the formula (7) for the Gibbs energy, entropy of the thin film can be found in the following form:

$$S = \frac{N}{2}k_B\sum_{l=a,b}\sum_{\nu=1}^{n}\ln\{2\exp\left[\beta\left(AQ_\nu^l + D\right)\right]\cosh\left[\beta\left(JM_\nu^l + h\right)\right] + 1\}$$

$$-\frac{N}{2}\frac{1}{T}\sum_{l=a,b}\sum_{\nu=1}^{n}m_\nu^l\left(JM_\nu^l + h\right) - \frac{N}{2}\frac{1}{T}\sum_{l=a,b}\sum_{\nu=1}^{n}q_\nu^l\left(AQ_\nu^l + D\right). \tag{22}$$

If we substitute Eq. (22) into (20) then the magnetic specific heat per one lattice site expressed in the Boltzmann constant units can be written as

$$\frac{C_h}{Nnk_B} = -\frac{1}{2}\sum_{l=a,b}\frac{1}{n}\sum_{\nu=1}^{n}\left[\left(\frac{\partial m_\nu^l}{\partial y}\right)_h\left(M_\nu^l + \frac{h}{J}\right) + \left(\frac{\partial q_\nu^l}{\partial y}\right)_h\left(\frac{A}{J}Q_\nu^l + \frac{D}{J}\right)\right]. \quad (23)$$

The quantities M_ν^l and Q_ν^l are given by the formulae (9) and (10), respectively.

The temperature derivatives of magnetization $\left(\partial m_\nu^l/\partial y\right)_h$ and the quadrupolar moment $\left(\partial q_\nu^l/\partial y\right)_h$ can be obtained after differentiating the respective set of equations in the form (5) and (6). Then we get the linear set of equations for the derivatives

$$y\left[\left(q_\nu^i\right)^2 - \left(m_\nu^i\right)^2\right]\left[z_{\nu,\nu}\left(\frac{\partial m_\nu^j}{\partial y}\right)_h + z_{\nu,\nu-1}\left(\frac{\partial m_{\nu-1}^j}{\partial y}\right)_h + z_{\nu,\nu+1}\left(\frac{\partial m_{\nu+1}^j}{\partial y}\right)_h\right]$$

$$-y^2 q_\nu^i\left(\frac{\partial m_\nu^i}{\partial y}\right)_h + y^2 m_\nu^i\left(\frac{\partial q_\nu^i}{\partial y}\right)_h$$

$$= \left[\left(q_\nu^i\right)^2 - \left(m_\nu^i\right)^2\right]\left[z_{\nu,\nu}m_\nu^j + z_{\nu,\nu-1}m_{\nu-1}^j + z_{\nu,\nu+1}m_{\nu+1}^j + \frac{h}{J}\right] \quad (24)$$

and

$$y\frac{A}{J}\left(1-q_\nu^i\right)\left[\left(q_\nu^i\right)^2 - \left(m_\nu^i\right)^2\right]$$

$$\times\left[z_{\nu,\nu}\left(\frac{\partial q_\nu^j}{\partial y}\right)_h + z_{\nu,\nu-1}\left(\frac{\partial q_{\nu-1}^j}{\partial y}\right)_h + z_{\nu,\nu+1}\left(\frac{\partial q_{\nu+1}^j}{\partial y}\right)_h\right]$$

$$+y^2 m_\nu^i\left(1-q_\nu^i\right)\left(\frac{\partial m_\nu^i}{\partial y}\right)_h - y^2\left[q_\nu^i - \left(m_\nu^i\right)^2\right]\left(\frac{\partial q_\nu^i}{\partial y}\right)_h$$

$$= \left(1-q_\nu^i\right)\left[\left(q_\nu^i\right)^2 - \left(m_\nu^i\right)^2\right]\left[\frac{A}{J}\left(z_{\nu,\nu}q_\nu^j + z_{\nu,\nu-1}q_{\nu-1}^j + z_{\nu,\nu+1}q_{\nu+1}^j\right) + \frac{D}{J}\right], \quad (25)$$

where $i = a, b$; $j = a + b - i$ and $\nu = 1, 2, \ldots, n$. In order to solve the above equations one has to calculate the magnetization distribution m_ν^l and the quadrupolar moments q_ν^l first and then to choose the physical solutions. These solutions for m_ν^l and q_ν^l are next treated as the input parameters in Eqs. (24) and (25). Once Eqs. (24) and (25) have been solved and the derivatives are determined, then from Eq. (23) we can calculate the magnetic specific heat in the thin film with arbitrary thickness.

3. The numerical results and discussion

The formulae derived in the previous section enable us the calculations of the susceptibility and specific heat vs. temperature, for the film with arbitrary thickness n (and for arbitrary parameters of single-ion anisotropy D/J and biquadratic interaction strength A/J). Among many possibilities for choice of these

parameters we will restrict ourselves to such situations which were discussed in the paper [24], i.e., $D/J = -0.7$ and $n = 5$, as the continuation from the point of view of magnetic response functions.

In Fig. 1, for our convenience, we recall the phase diagram obtained in our previous paper [24] for the film with $n = 5$. The diagram is plotted in the co-ordinates $(A/J, k_BT/J)$ for fixed value of single-ion anisotropy $D/J = -0.7$. For comparison, in the same figure the diagrams for single atomic layer ($n = 1$) and for bulk material ($n = \infty$) are also shown. We see that the thin film with $n = 5$ and free surfaces is an intermediate situation between $n = 1$ and $n = \infty$, and the phase diagram does not differ much from the bulk material. The lines in the diagram separate the regions where the particular phases, namely: ferromagnetic (F), paramagnetic (P) and staggered quadrupolar (SQ) are energetically favourable. The solid lines denote the continuous (II-nd order) phase transitions, whereas the dashed lines correspond to the discontinuous (I-st order) ones. As we can see, the I-st order phase transitions occur between SQ and F phases as well as between F and P. With the bold dots we marked the tricritical points, where the continuous phase transitions lines meet the discontinuous boundary. The values of these tricritical points for $n = 1$, 5 and ∞ are contained in Table.

As it was discussed in the paper [24] such a kind of the phase diagram represents an intermediate situation between the pure BEG model (when $D = 0$) and Blume–Capel (BC) model (when $A = 0$). The characteristic feature is the

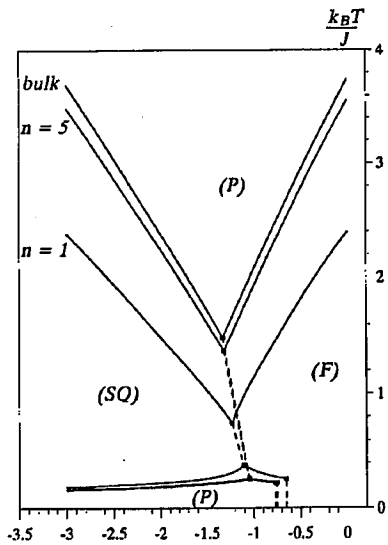

Fig. 1. Phase diagram of a thin film with $n = 5$ plotted in (T, A)-plane for $D/J = -0.7$. Solid lines represent the continuous phase transitions, whereas dashed lines correspond to the discontinuous (I-st order) ones. By bold dots we denoted tricritical points. The ranges of existence for F, P and SQ phases are shown. For comparison, the phase diagrams for $n = 1$ and $n = \infty$ are also depicted.

TABLE

The coordinates of tricritical points from the diagrams corresponding to $n = 1$, 5 and $n = \infty$ ($D/J = -0.7$). The tricritical points are represented by the full dots in Fig. 1.

$D/J = -0.7$	A/J	$k_B T_c/J$
$n = 1$	- 1.229	0.744
	- 1.105	0.380
	-0.649	0.257
$n = 5$	-1.318	1.377
	-1.049	0.262
	-0.75	0.223
bulk	-1.331	1.491
	-1.044	0.252
	-0.766	0.219

occurrence of P phase at low temperatures. Such P phase at higher temperatures is replaced by more ordered one, i.e. SQ or F phase, depending on the value of A parameter.

The magnetization and quadrupolar moment dependencies vs. temperature for such kind of the phase diagram were discussed in [24] in detail. Below, in Figs. 2–5, we present the isothermal susceptibility χ_T vs. dimensionless temperature $y = k_B T/J$, for four values of A parameter, representing the biquadratic interactions. Namely, we chose $A/J = 0; -0.9; -1.1$ and -1.35 for Figs. 2–5, respectively, whilst $D/J = -0.7 = \text{const}$ for all figures. Such choice of parameters gives the most interesting cross-sections for the phase diagram (Fig. 1) and illustrates the influence of biquadratic interactions on the susceptibility.

Next, in Figs. 6–9 we present the magnetic specific heat C_h (for $h = 0$) vs. dimensionless temperature y. The calculations illustrated in Figs. 6–9 are performed for the same parameters n, A and D as for the susceptibility (Figs. 2–5, respectively). In all figures (2–9) the solid curves represent the temperature dependencies of either χ_T or C_h, whereas the dashed lines are drawn to denote the phase transitions temperatures. Now, we will analyse Figs. 2–9 in detail.

In Fig. 2 the isothermal susceptibility χ_T is drawn for $A = 0$ and $D/J = -0.7$. The situation is then characteristic of a pure BC model (compare with Fig. 1 for $A/J = 0$). In this case only one (continuous) phase transition is present. It takes place between F and P phases for $y = 3.564$. As we expect, at the phase transition temperature the susceptibility χ_T has the singularity and tends to zero far away from this point, i.e., when $T \to 0$ or $T \to \infty$.

In Fig. 3 we present the χ_T dependence vs. temperature for $A/J = -0.9$ and $D/J = -0.7$. As we noted from Fig. 1, for such parameters two continuous phase transitions can be expected; namely, from P to F phase at $y = 0.241$, and from P

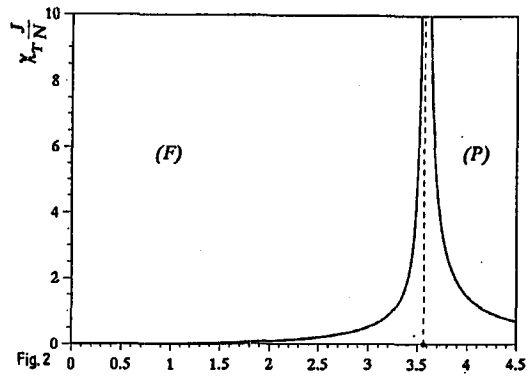

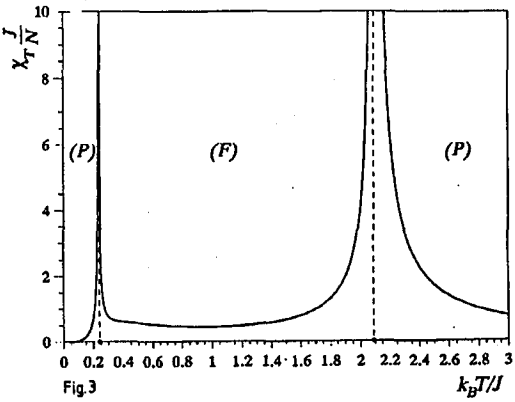

Fig. 2. The isothermal susceptibility χ_T vs. temperature for $n = 5$, $A/J = 0$ and $D/J = -0.7$. In all next figures (2–9) thin dashed lines denote the phase transitions temperatures.

Fig. 3. The isothermal susceptibility χ_T vs. temperature for $n = 5$, $A/J = -0.9$ and $D/J = -0.7$.

to F phase at $y = 2.089$. At these two transition points the susceptibility diverges, but it can be noted that the peak for lower temperature is narrower.

In the next figure (Fig. 4) we plot χ_T vs. y for $A/J = -1.1$ ($D/J = -0.7$). From Fig. 1 we can see that for these parameters three different phase transitions should appear. Figure 4 confirms this conclusion. At first, the continuous phase transition from P to SQ phase takes place at $y = 0.253$, which is accompanied by the finite peak of the susceptibility. Then, the I-st order transition between SQ and F phase appears at $y = 0.477$. However, in this case the susceptibility has no maximum. Instead, the discontinuous behaviour is present. The last transition (continuous) between F and P phases occurs at $y = 1.749$ and is of the same character as that previously described in Figs. 2 and 3. In Fig. 4, as well as in the next Fig. 5, we plotted two susceptibilities in SQ phase (the dashed lines), which correspond to a and b sublattices, respectively. As we know, the SQ phase is characterized by the solutions $m_\nu^a = m_\nu^b = 0$ and $q_\nu^a \neq q_\nu^b$ [24] and this fact gives

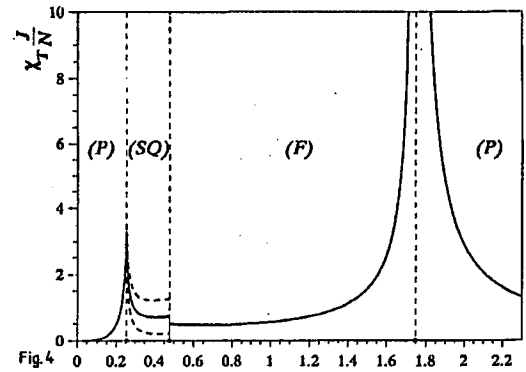

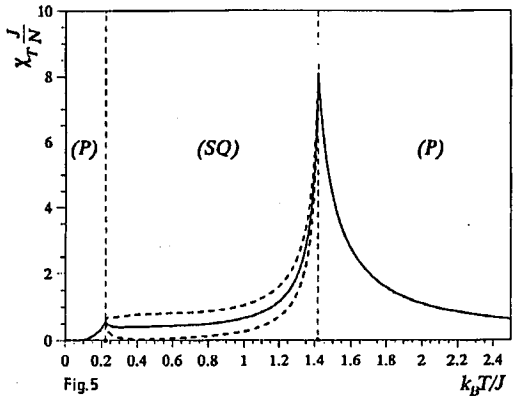

Fig. 4. The isothermal susceptibility χ_T vs. temperature for $n = 5$, $A/J = -1.1$ and $D/J = -0.7$. For SQ phase by thick dashed lines we denoted the susceptibilities of two interpenetrating sublattices, whereas the solid thick line represents the mean value of these two susceptibilities.

Fig. 5. The isothermal susceptibility χ_T vs. temperature for $n = 5$, $A/J = -1.35$ and $D/J = -0.7$.

rise to the appearance of two different susceptibilities. The solid curve in SQ phase represents the mean value of these two solutions.

In Fig. 5, the susceptibility χ_T is plotted vs. y for $A/J = -1.35$ ($D/J = -0.7$). For such values of parameters two phase transitions should appear (see Fig. 1). Firstly, we have the phase transition between P and SQ phase at $y = 0.223$ and next, the transition from P to SQ phase at $y = 1.418$. Both these transitions are continuous and are accompanied by the finite peaks of susceptibility. It can be noted that the relative height of both peaks changes for different A/J. Namely, when A/J decreases, the high-temperature (right) peak decreases faster than the low-temperature (left) peak, therefore it can become even lower than the left one. Such situation is observed, for instance, when $A/J = -2.5$. The susceptibility in SQ phase is represented in Fig. 5 by two sublattice susceptibilities (the dashed curves) and their mean value is shown, analogously to Fig. 4.

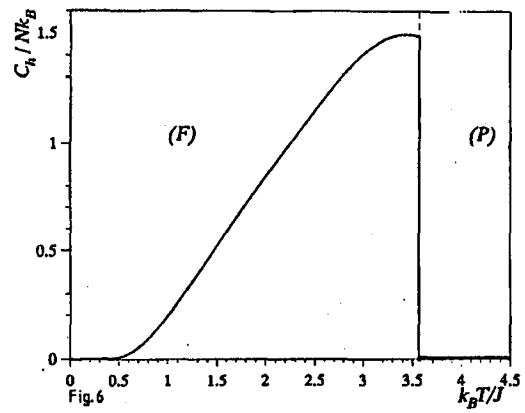

Fig.6

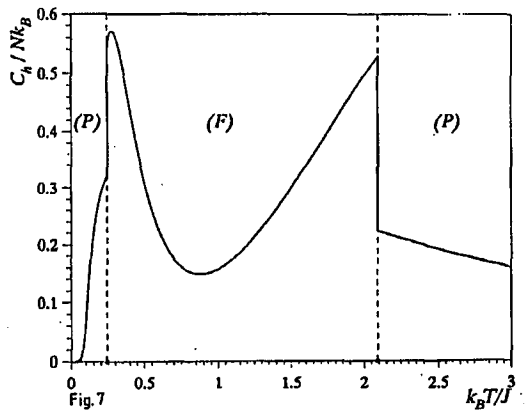

Fig.7

Fig. 6. The magnetic specific heat C_h vs. temperature for $n = 5$, $A/J = 0$ and $D/J = -0.7$. The parameters are the same as in Fig. 2.
Fig. 7. The magnetic specific heat C_h vs. temperature for $n = 5$, $A/J = -0.9$ and $D/J = -0.7$ (compare with Fig. 3).

Figures 2–5 illustrate the most characteristic situations from the phase diagram (Fig. 1) and show the isothermal susceptibility in three different phases, P, F, and SQ. In the next figures we will illustrate the magnetic specific heat (for $h = 0$) for the same situations as in the case of susceptibility.

In Fig. 6 we show the specific heat C_h vs. y for $A/J = 0$ and $D/J = -0.7$, i.e., the parameters are the same as for Fig. 2. The specific heat increases from zero value at $y = 0$ and slightly before the phase transition temperature it reaches a soft maximum. At T_c ($y = 3.564$) the jump of the specific heat is observed to nearly zero value in the paramagnetic phase. The small specific heat remainder in P phase can be attributed to the quadrupolar moment dependence vs. temperature for spin $S = 1$. It is worth noticing here that for spin $S = 1/2$ (in MFA) the specific heat in P phase is strictly equal to zero.

Figure 7 shows the C_h curve for the parameters $A/J = -0.9$ ($D/J = -0.7$) which correspond to Fig. 3. Two II-nd order phase transitions are then observed,

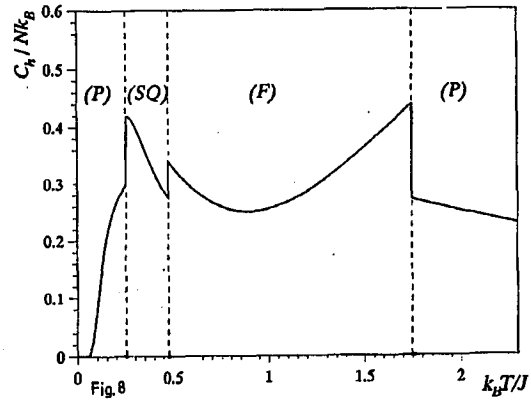

Fig. 8

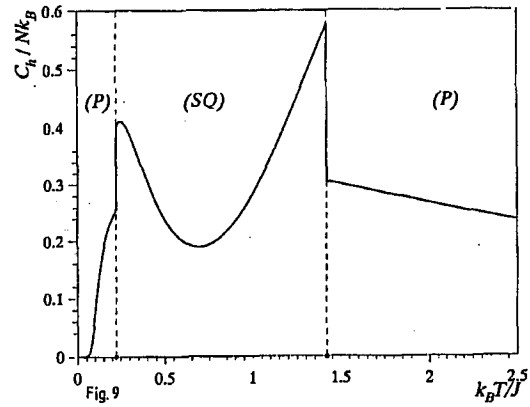

Fig. 9

Fig. 8. The magnetic specific heat C_h vs. temperature for $n = 5$, $A/J = -1.1$ and $D/J = -0.7$. For SQ phase we plotted the mean value of specific heat from the two sublattices (compare with Fig. 4).

Fig. 9. The magnetic specific heat C_h vs. temperature for $n = 5$, $A/J = -1.35$ and $D/J = -0.7$ (compare with Fig. 5).

which is typical of the re-entrant magnetism phenomenon [24]. For both these transitions the specific heat shows a jump from the lower value in P phase to a higher value in the ordered F phase. Then, for the intermediate temperatures in F phase the specific heat has a minimum. By comparison with Fig. 6 we can conclude that the specific heat in high-temperature P phase is here much greater than for $A = 0$. This remarkable increase in the specific heat in P phase is due to the role of biquadratic interactions.

Further, in Fig. 8 the specific heat is shown for $A/J = -1.1$ ($D/J = -0.7$) and the choice of parameters corresponds to Fig. 4. Three phase transitions are then observed, each of them is represented by the discontinuous jump of the specific heat. As a rule, at each transition point the specific heat of a more ordered phase is higher than that for the less ordered phase (i.e., with higher symmetry). The

specific heat in the SQ phase varies quite rapidly with temperature and it has a relatively high value. However, the SQ phase in Fig. 8 exists only in a narrow temperature range between P and F phases. Therefore it is interesting to see what happens when this phase extends over a wide temperature range.

Figure 9 illustrates a situation when $A/J = -1.35$ ($D/J = -0.7$). Such choice of parameters corresponds to Fig. 5. The SQ phase is then surrounded by two P phases and both phase transitions are continuous from the point of view of quadrupolar moment. As in the previous figures, the jumps of the specific heat at phase transition temperatures occur, moreover, in SQ phase the specific heat has a broad minimum. Qualitatively, Fig. 9 is similar to Fig. 7. Although, instead of the F phase in Fig. 7 we have here the staggered quadrupolar phase with $m = 0$ but with the analogous behaviour of the specific heat. In all figures 6–9 the specific heat in high-temperature P phase has a remarkable value due to the presence of biquadratic interactions.

4. Final remarks

The results obtained for the susceptibility and specific heat, presented in Figs. 2–9, concern a thin film in BEG model. However, most of the properties discussed here should appear not only in thin films but also in the bulk material, since the phase diagrams are quite similar (see also [24]). For instance, two sublattice susceptibilities in SQ phase should be a general property of BEG model. As far as we know, this fact has never been discussed in literature.

The final result for the susceptibility in the thin film, is taken as a sum from all atomic planes. We presume that the susceptibility of a particular ν-th plane is not a quantity measurable separately. However, one has to point out that we naturally calculate the susceptibility profile across the film, similarly to the profile of magnetization or quadrupolar moment [24]. As far as the specific heat is concerned, in the numerical calculations we restricted ourselves to the case of $h = 0$. Formally, from our formulae we can separate the specific heat for a and b sublattice, however we think that only a summary heat can be measurable and therefore only such a quantity is plotted on the graphs. For all kinds of phase transitions considered here, both continuous and discontinuous, the specific heat changes discontinuously. We would like to point out that the specific heat of disordered P phase, calculated here in MFA for the spin $S = 1$ case, is not equal to zero as it is for the case of spin $S = 1/2$. The reason is that the temperature derivatives of the quadrupolar moment, $\partial q/\partial y$, occurring in Eq. (23) are not equal to zero in the presented model.

Both magnetic response functions, i.e., χ_T and C_h, tend to zero when $T \to 0$. The vanishing of C_h is in accordance with the third law of thermodynamics. Both these functions were obtained from the same root: the Gibbs free energy of the thin film [24]. Therefore, we can conclude from this paper (and from [24]) that the thermodynamic properties of the BEG film can be completely described within our method. We would like to mention that we restricted ourselves in the numerical calculations to the region $D < 0$ and $A < 0$. This region is the most interesting from the point of view of discontinuous phase transitions and tricritical point trajectory [25].

The authors are aware of the fact that the molecular field approximation can be treated as nonsatisfactory, particularly when one takes into account some differences for the bulk phase diagrams obtained in MFA and compared with more accurate methods like cluster variational method in pair approximation (CVMPA) [22] or Monte Carlo [2, 3]. However, as far as the thin films are concerned, the application of the latter methods is still a matter of future. Therefore, the MFA results obtained in the present paper could serve as a reference point when more advanced methods for the films are available.

References

[1] M. Blume, V.J. Emery, R.B. Griffiths, *Phys. Rev. A* **4**, 1071 (1971).

[2] M. Tanaka, T. Kawabe, *J. Phys. Soc. Jap.* **54**, 2194 (1985).

[3] Y.L. Wang, C. Wentworth, *J. Appl. Phys.* **61**, 4411 (1987).

[4] T. Kaneyoshi, *J. Phys. Soc. Jap.* **56**, 4199 (1987).

[5] J.W. Tucker, *J. Magn. Magn. Mater.* **71**, 27 (1987).

[6] T. Kaneyoshi, E.F. Sarmento, I.P. Fittipaldi, *Suppl. to Trans. Jap. Inst. Metals* **29**, 395 (1988).

[7] J.W. Tucker, *J. Phys. Condens. Mater.* **1**, 485 (1989).

[8] J.W. Tucker, *J. Magn. Magn. Mater.* **80**, 203 (1989).

[9] W. Hoston, A.N. Berker, *Phys. Rev. Lett.* **67**, 1027 (1991).

[10] C. Buzano, A. Pelizzola, *Physica A* **189**, 333 (1992).

[11] C. Buzano, A. Pelizzola, *Physica A* **195**, 197 (1993).

[12] A. Rosengren, S. Lapinskas, *Phys. Rev. B* **47**, 2643 (1993).

[13] R.R. Netz, A.N. Berker, *Phys. Rev. B* **47**, 15019 (1993).

[14] R.J.C. Booth, Lu Hua, J.W. Tucker, C.M. Care, I. Halliday, *J. Magn. Magn. Mater.* **128**, 117 (1993).

[15] J.A. Plascak, J.G. Moreira, F.C. Sá Barreto, *Phys. Lett. A* **173**, 360 (1993).

[16] S. Lapinskas, A. Rosengren, *Phys. Rev. B* **49**, 15190 (1994).

[17] M. Kerouad, M. Saber, J.W. Tucker, *J. Magn. Magn. Mater.* **146**, 47 (1995).

[18] S. Sardar, K.G. Chakraborty, *Physica A* **206**, 544 (1994).

[19] D.L. Lin, Hao Che, Wei Lai, T.F. George, *Phys. Rev. E* **49**, 2155 (1994).

[20] T. Balcerzak, J.W. Tucker, *J. Magn. Magn. Mater.* **140-144**, 653 (1995).

[21] C. Buzano, A. Pelizzola, *Physica A* **216**, 158 (1995).

[22] D. Wingert, D. Stauffer, *Physica A* **219**, 135 (1995).

[23] M. Jascur, T. Kaneyoshi, *Phys. Status Solidi B* **174**, 537 (1992).

[24] T. Balcerzak, M. Gzik, *Acta Phys. Pol. A* **91**, 293 (1997).

[25] T. Balcerzak, M. Gzik, *Phys. Status Solidi B* **199**, 541 (1997).